Cell

Activation of STAT6 by STING Is Critical for Antiviral Innate Immunity

Huihui Chen,[1,2,6] Hui Sun,[1,2,6] Fuping You,[1,2,6] Wenxiang Sun,[1,2] Xiang Zhou,[1,2] Lu Chen,[1,2] Jing Yang,[1,2] Yutao Wang,[1,2] Hong Tang,[1,2] Yukun Guan,[1,2] Weiwei Xia,[1] Jun Gu,[1] Hiroki Ishikawa,[4] Delia Gutman,[4] Glen Barber,[4] Zhihai Qin,[5] and Zhengfan Jiang[1,2,3,*]
[1]State Key Laboratory of Protein and Plant Gene Research
[2]Key Laboratory of Cell Proliferation and Differentiation of the Ministry of Education
School of Life Sciences, Peking University, Beijing, China
[3]Peking University-Tsinghua University Joint Center for Life Sciences, Beijing, China
[4]Department of Medicine and Sylvester Comprehensive Cancer Center, University of Miami School of Medicine, Miami, FL 33136, USA
[5]State Key Laboratory of Biomacromolecules, Institute of Biophysics, Beijing, China
[6]These authors contributed equally to this work
*Correspondence: jiangzf@pku.edu.cn
DOI 10.1016/j.cell.2011.09.022

SUMMARY

STAT6 plays a prominent role in adaptive immunity by transducing signals from extracellular cytokines. We now show that STAT6 is required for innate immune signaling in response to virus infection. Viruses or cytoplasmic nucleic acids trigger STING (also named MITA/ERIS) to recruit STAT6 to the endoplasmic reticulum, leading to STAT6 phosphorylation on Ser^{407} by TBK1 and Tyr^{641}, independent of JAKs. Phosphorylated STAT6 then dimerizes and translocates to the nucleus to induce specific target genes responsible for immune cell homing. Virus-induced STAT6 activation is detected in all cell-types tested, in contrast to the cell-type specific role of STAT6 in cytokine signaling, and *Stat6*$^{-/-}$ mice are susceptible to virus infection. Thus, STAT6 mediates immune signaling in response to both cytokines at the plasma membrane, and virus infection at the endoplasmic reticulum.

INTRODUCTION

Innate immunity is the first line of defense against microbial infection. Recognition of pathogens is mainly mediated by pattern recognition receptors (PRRs), including Toll-like receptors (TLRs), RIG-I-like receptors (RLRs) and NOD-like receptors (NLRs) (Takeuchi and Akira, 2010), that trigger signal cascades to upregulate the expression of various cytokines. In the case of viral infection, endosomal TLRs and cytoplasmic RLRs detect viral DNAs or RNAs and induce the production of type I IFN, which are potent inhibitors of viral replication (Gitlin et al., 2006; Kato et al., 2005, 2006). RLRs, including RIG-I and Mda5, are sensors of viral RNAs in the cytoplasm; in response to viral infection, RLRs associate with the adaptor protein MAVS/Cardif/IPS-1/VISA (Kawai et al., 2005; Meylan et al., 2005; Seth et al., 2005; Xu et al., 2005), an integral membrane protein that functions on both mitochondria and peroxisomes through distinct mechanisms (Dixit et al., 2010); the RLR/MAVS complex facilitates TBK1/IKKε-mediated activation of IRF3/7 and NF-κB, which lead to the induction of type I IFNs. Besides viral RNA, cytoplasmic double-stranded DNA (dsDNA) also induces type I IFNs, but the exact identity of the receptor in this situation is currently not fully established (Ishii et al., 2006; Stetson and Medzhitov, 2006). A recently identified adaptor protein, endoplasmic reticulum IFN stimulator (STING, also named MITA/ERIS) (Ishikawa and Barber, 2008; Sun et al., 2009; Zhong et al., 2008) exhibits a vital role in dsDNA signaling (Ishikawa et al., 2009). The DNA sensors induce type I IFN production either through STING (IFI16 [Unterholzner et al., 2010]) or via the RIG-I–MAVS axis (involving RNA polymerase III mediated transcription of cytoplasmic DNA [Ablasser et al., 2009; Chiu et al., 2009]), and both pathways ultimately result in the recruitment and activation of TBK1, which in turn activates IRF3/7 and NF-κB.

Many cytokines, including type I IFNs, exert their effects through the canonical JAK (Janus kinase)-STAT (signal transducers and activators of transcription) pathway (Levy and Darnell, 2002). Specifically, IL-4 and IL-13 activate STAT6 (Takeda et al., 1996) resulting in T helper cells 2 (T_h2) polarization (Akimoto et al., 1998; Hebenstreit et al., 2006; Shimoda et al., 1996). IL-4 induces the phosphorylation of IL-4 receptor, which in turn recruits cytosolic STAT6 by its SH2 domain; the recruited STAT6 is phosphorylated on tyrosine 641 (Y^{641}) by JAK1, which results in the dimerization and nuclear translocation of STAT6 to activate target genes (Mikita et al., 1996, 1998). Several cytokines, including IL-3/15, IFN-α and platelet-derived growth factor (PDGF-BB), activate STAT6 in different cell types (Bulanova et al., 2003; Masuda et al., 2000; Quelle et al., 1995), and induce over 150 diverse targets, many of which are involved in T_h2-associated processes (Elo et al., 2010; Wei et al., 2010). A thorough understanding of biological consequences of STAT6 signaling awaits additional studies.

It is known that NF-κB, AP-1 and IRFs are responsible for the induction of many IFN-stimulated genes (ISGs), however, the role of STAT6 in anti-viral response is unclear. Here we report a STAT6-dependent antiviral innate immune signaling event

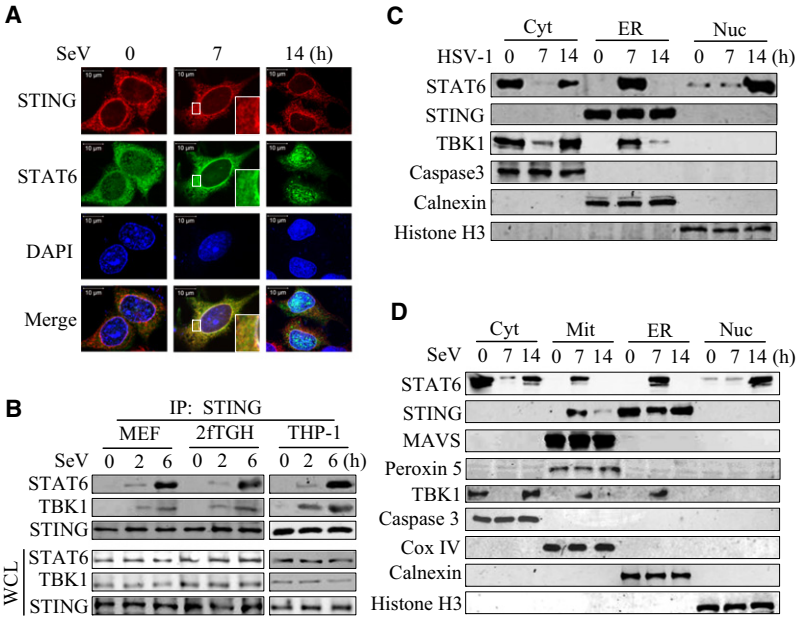

Figure 1. Virus-Induced STAT6-STING Interaction and STAT6 Translocation

(A) STAT6 translocates and colocalizes with STING after virus infection. Confocal microscopy of endogenous STING (red), STAT6 (green) and the merge in HeLa cells infected with Sendai virus (SeV) for the indicated hours. Nuclei were stained with DAPI. All images are representative of at least three independent experiments in which >95% of the cells displayed similar staining. Scale bars represent 10 μm.

(B) STAT6 interacts with STING and TBK1 after virus infection. Primary MEFs, 2fTGH and THP-1 cells were infected with SeV for the indicated hours. Cell lysates were immunoprecipitated (IP) with α-STING and blotted (IB) with STAT6, TBK1 and MAVS antibodies. WCL, whole cell lysates.

(C and D) Virus infection induces STAT6 translocation. Western blot analyses of fractionated HeLa cells infected with Herpes simplex virus 1 (HSV-1) (C) or SeV (D) for the indicated hours. Cyt, cytosolic; ER, endoplasmic reticulum-rich; Nuc, nuclear; and Mit, mitochondrial; were revealed by Caspase 3, Calnexin, Histone H3, and COX IV, respectively.

See also Figure S1.

that leads to the induction of chemokines, including CCL2, CCL20, and CCL26, and these chemokines recruit immune cells to combat viral infection. More importantly, virus induces STAT6 activation independently of JAK, but instead relies on STING and TBK1, as well as MAVS in the case of RNA virus. The physiological significance of the novel pathway is reflected by a higher susceptibility of *Stat6*$^{-/-}$ mice to viral infections; moreover, unlike other cell type-specific STAT6 signaling pathways, virus-induced STAT6 activation is ubiquitously detected, implying a fundamental requirement of this mechanism in the defense against viral infections.

RESULTS

STAT6 Interacts with STING in Response to Virus Infection

Using C-terminal STING (aa 178–379) as bait in the yeast 2-hybrid screen, we identified an STING-STAT6 interaction and confirmed it in 293 cells by coimmunoprecipitation (coIP) (Figure S1A available online). Specifically, the DNA-binding domain (DBD) of STAT6 and STING C terminus (aa 317–379) were required for this interaction (Figures S1B–S1D). We next examined this interaction at endogenous protein levels. Analysis with confocal microscope showed a dispersed pattern of STAT6 in the cytosol of unstimulated HeLa cells; upon infection with Sendai virus (SeV, an RNA virus), STAT6 redistributes to the perinuclear regions, colocalizes with STING, and eventually translocates into the nucleus (Figure 1A). CoIP analyses also revealed an inducible interaction of endogenous STAT6 with STING, as well as MAVS and TBK1, in SeV-infected primary MEFs, 2fTGH and THP-1 cells (Figure 1B). Consistent with these observations, endogenous STAT6 co-fractionate with STING in HeLa cell lysates after Herpes simplex virus 1 (HSV-1, a DNA virus) infection (Figure 1C). Similar results were obtained from SeV-infected HeLa cells, with an additional location to a mixed fraction containing MAVS-resident mitochondria-associated ER membrane (MAM) and also MAVS-resident peroxisomal membrane (Dixit et al., 2010; Ishikawa et al., 2009; Zhong et al., 2008) (Figure 1D). These data demonstrate that STAT6 interacts with STING during virus infection.

STAT6 Is Activated upon Virus Infection

293 cells lack a functional endogenous STAT6 but express the other components of the IL-4 signaling pathway (Mikita et al., 1996, 1998). Taking advantage of this property, we first established a 293 cell-line stably expressing Flag-STAT6 (293-STAT6) and confirmed its normal responsiveness to IL-4/13 with intact Y^{641} phosphorylation (data not shown). Virus infection resulted in the nuclear translocation of STAT6, suggesting that STAT6 may serve as a transcriptional activator under this situation. To confirm this hypothesis, we assessed Y^{641} phosphorylation of STAT6, since it is required for STAT6 activation in response to cytokines. We found that STAT6 was indeed phosphorylated on Y^{641} in SeV-infected and poly (I:C)/poly dAdT-transfected cells, and this STAT6 phosphorylation takes place prior to the phosphorylation of IRF3 and other STATs (Figures 2A, 2D, and 2H, and Figures S2B and S2H). A STAT6-responsive luciferase reporter (E3-Luc) (Yuan et al., 2006) was activated in 293-STAT6 cells upon virus infection and poly (I:C)/poly dAdT transfection, whereas a nonresponsive control reporter (mutated at the STAT6-binding site, E3-Luc-M) was not affected (Figure 2C and Figure S2A). By contrast, neither reporter was activated in 293 cells, indicating a transactivation function of STAT6 in response to virus. These findings imply a previously unknown pathway of STAT6 activation in response to viral infection and cytoplasmic dsRNA/DNA.

STAT6 can be activated by several cytokines. To clarify a potential role of cytokines in STAT6 activation during viral challenges, we first monitored cytokine production in virus-infected cells. Neither IL-4 nor IL-13 was induced by virus (Figure 2B

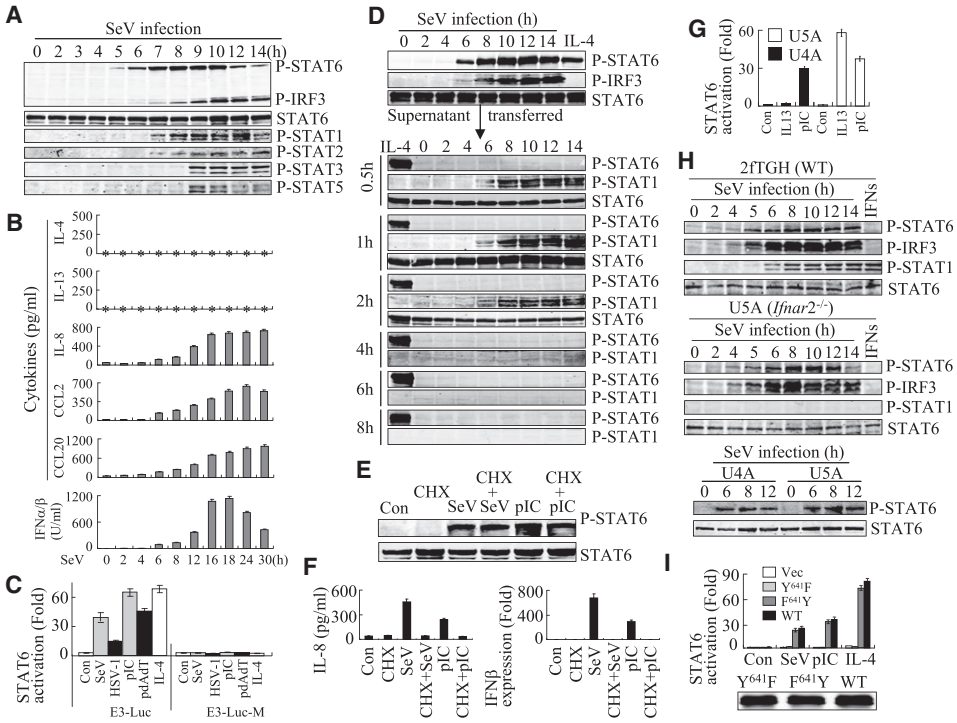

Figure 2. Virus-Induced STAT6 Activation

(A) SeV induces STAT6 phosphorylation. 293-STAT6 cells were infected with SeV for the indicated hours. Phosphorylation of the indicated proteins was analyzed by western blot. (Top panel: membrane was probed with α-P-STAT6, developed, and reprobed with α-P-IRF3.)

(B) Kinetics of cytokine induction by virus. Supernatants of cells in (A) and prolonged infected-cells as indicated were subject to ELISA or type I IFN bioassay. Asterisk indicates levels that were not detectable.

(C) Virus infection activates STAT6. 293-STAT6 cells transfected with an E3-Luc (STAT6-responsive reporter) or E3-Luc-M (STAT6-nonresponsive reporter) were treated with IL-4 for 12 hr, transfected with poly (I:C) (pIC)/poly dAdT (pdAdT) or infected with SeV/HSV-1 for 24 hr. STAT6 activation was analyzed using luciferase assay (fold induction).

(D) Virus-induced STAT6 activation is independent of cytokines in culture media. Naive 293-STAT6 cells were incubated with supernatants from SeV-infected 293-STAT6 cells for indicated times. Both infected (upper panels) and media-treated cells (lower panels) were analyzed for phosphorylation of the indicated proteins by western blot. Lysate from IL-4 treated cells was used as a positive control for STAT6 phosphorylation detection.

(E) Virus-induced STAT6 phosphorylation does not require protein synthesis. Mock or cycloheximide (CHX, 5 μg/ml) pretreated (for 2 hr) 293-STAT6 cells were infected with SeV or transfected with poly (I:C) for 10 hr. STAT6 phosphorylation was analyzed by western blot.

(F) Left, ELISA analyses of IL-8 production in supernatants of cells treated in (E) for 24 hr. Right, IFN-β-Luc reporter assay for the induction of IFN-β in the same cells.

(G) JAK1 and IFNAR2 are not required for STAT6 activation by virus. U4A (*JAK1*$^{-/-}$) and U5A (*IFNAR2*$^{-/-}$) cells transfected with an E3-Luc were treated with IL-13 for 12 hr or transfected with poly (I:C) for 24 hr. STAT6 activation was analyzed using luciferase assay (fold induction).

(H) JAK1 and IFNAR2 are not required for STAT6 phosphorylation by virus. 2fTGH, U4A and U5A cells were infected with SeV for the indicated hours. Phosphorylation of the indicated proteins was analyzed by western blot. IFNs, 2 hr of type I IFNs (500 unit/ml IFN-α & 500 unit/ml IFN-β) treatment.

(I) Y^{641} phosphorylation is a prerequisite for STAT6 activation. 293 cells transfected with an E3-Luc and wild-type (WT) or mutant STAT6 were infected with SeV, transfected with poly (I:C) for 24 hr or treated with IL-4 for 12 hr. Luciferase activity was analyzed as fold induction (upper panel). Vec, empty vector; $F^{641}Y$, the reversed $Y^{641}F$. Expression of STAT6 was analyzed by western blot (lower panel).

Data are means ± SEM. See also Figure S2.

and Figure S2C), thus excluding their involvement in STAT6 activation after virus infection. Strikingly, other cytokines including type I IFNs, IL-8 and STAT6-induced genes (CCL2 and CCL20, see below), displayed similar kinetics post infection. Therefore, CCL2/20 is unlikely regulated by cytokines like type I IFNs or IL-8. In fact, when media of SeV-infected 293-STAT6 cells were used to treat naive 293-STAT6 cells, STAT6 phosphorylation was only detected in virus-infected but not media-treated cells, whereas phosphorylation of STAT1/2/3/5 was detected in media-treated cells (Figure 2D and data not shown), excluding any STAT6-activating cytokines in the media within these time points. Furthermore, STAT6 phosphorylation was intact upon SeV and poly (I:C) stimulation when production of cytokines including IL-8 and type I IFNs was inhibited by cycloheximide (CHX) pretreatment (Figures 2E and 2F). These data collectively indicate a cytokine –independent pathway of STAT6 activation upon virus infection.

Next we used 2fTGH and its derivative cell lines (Kumar et al., 1997) (each deficiency in a single key component of the JAK–STAT pathway, Figure S2D) to test if any of these known proteins in JAK-STAT pathway would be required for virus-induced STAT6 activation. Notably, U4A cells with JAK1 deficiency did

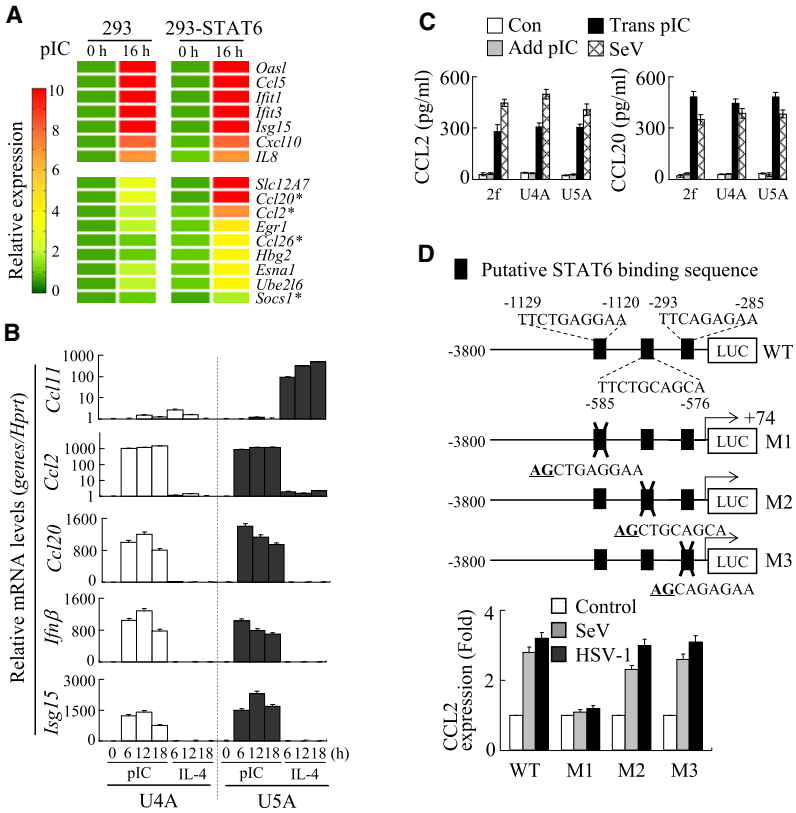

Figure 3. Virus-Activated STAT6 Regulates Specific Target Genes

(A) Microarray analysis of poly (I:C)-induced genes. Expression levels in 293 cells were arbitrarily set to 1 (green). Heat map of genes most strongly upregulated by poly (I:C) in both cells (top) and only in 293-STAT6 cells (bottom). Stars indicate genes confirmed by quantitative–PCR, western blot and/or ELISA.

(B) Quantitative–PCR analyses of U4A and U5A cells transfected with poly (I:C) or treated with IL-4 for the indicated hours. Data were normalized to the relative expression of the *HPRT1* reference gene.

(C) CCL2 and CCL20 are upregulated in the absence of JAK1 or IFNAR2. ELISA analyses of 2fTGH (2f), U4A and U5A cells transfected with poly (I:C) (Trans pIC), treated with poly (I:C) (Add pIC) or infected with SeV for 24 hr.

(D) *CCL2* promoter contains a functional STAT6 site that is responsive to virus infection. A schematic presentation of STAT6 binding site mutants is shown (upper). 293-STAT6 cells transfected with the indicated promoter-reporters were infected with SeV or HSV-1. Luciferase activity was analyzed as fold induction.

Data are means ± SEM. See also Figure S3.

not respond to IL-4/13 (Figure 2G and Figures S2D–S2G), while U5A cells deficient in IFNAR2 were completely defective in IFN-α/β response (Figure S2F). Surprisingly, STAT6 from all these cells responded normally to virus infection (Figures 2G and 2H and Figure S2G), indicating that none of these components alone is indispensable. Besides, cytokine effects were re-examined using these cells. Treatment with a high concentration of IFNs and other STAT6-responding cytokines including IL-3/15 and PDGF-BB did not result in STAT6 phosphorylation in 2fTGH or U5A cells (Figure 2H, Figure S2F, and data not shown), supporting our previous conclusion that virus-induced STAT6 activation is cytokine-independent.

Although virus-induced STAT6 activation appears to be quite different from that induced by IL-4/13, Y^{641} phosphorylation is essential for both activation pathways since mutation of this residue totally abolished its response to virus or IL-4/13 (Figure 2I). The SH2 domain of STATs is essential not only for both receptor-binding and dimerization, but is also required for DNA binding by this family of proteins. To investigate the role of SH2 domain in virus-induced STAT6 activation, we searched for potential residue(s) in this domain that might be important. We found that $L^{551}A$ mutant lost the ability to respond to virus, albeit with normal response to IL-4/13, and the defect was fully rescued by the reversion mutation (Figures S2I–S2L). Further experiments showed that the $L^{551}A$ mutation abrogated Y^{641} phosphorylation and STAT6 homo-dimerization in response to virus; by contrast, the mutation has no effect on STAT6 activation by IL-4 (Figures S2M-S2O). Collectively these data suggest that STAT6 is differentially activated by virus and IL-4/13.

Virus-Activated STAT6 Regulates a Specific Set of Target Genes

Using DNA microarrays, we compared mRNAs that are significantly induced in mock or poly (I:C) transfected 293 and 293-STAT6 cells. Among 30, 968 genes examined, poly (I:C) transfection induced the expression of numerous ISGs in both cells, including *OAS1*, *CCL5* and *IFIT1/3*, and a set of genes only in 293-STAT6 cells (Figure 3A), suggesting that these genes are specifically regulated by STAT6; notably among the STAT6-regulated genes are the chemokines *CCL2*, *CCL20*, and *CCL26*, which are responsible for the recruitment of immune cells to sites of infection. The microarray data were validated by either quantitative–PCR or ELISA (Figures 3B and 3C and Figure S3), respectively.

The transcriptome of poly (I:C) stimulated 293-STAT6 cells displayed substantial difference from that of IL-4/13 activated cells. In fact, while *CCL11* was only upregulated by IL-4 treatment, *CCL26* could be induced by both IL-4 and virus. Consistently, both SeV and poly (I:C) were able to induce *CCL2* and *CCL20* in U4A and U5A cells (Figures 3B and 3C). Furthermore, inspection of *CCL2* promoter sequence revealed one typical and two putative STAT6 binding sites (–1129 to –1120, –585 to –576, and –293 to –285 relative to the transcriptional start site, respectively). SeV and HSV-1 infection indeed activated a luciferase reporter driven by DNA segment containing these sites, but not the one with mutation in the first STAT6 binding site (Figure 3D), suggesting that *CCL2* promoter harbors a functional STAT6 binding site that is responsive to virus infection.

STING Mediates STAT6 Activation by Virus

Next, we sought to investigate the molecular mechanism of STAT6 signaling in response to virus. The translocation and interaction of STAT6 with STING after virus infection (Figure 1) raised the possibility that STING is involved in STAT6 activation.

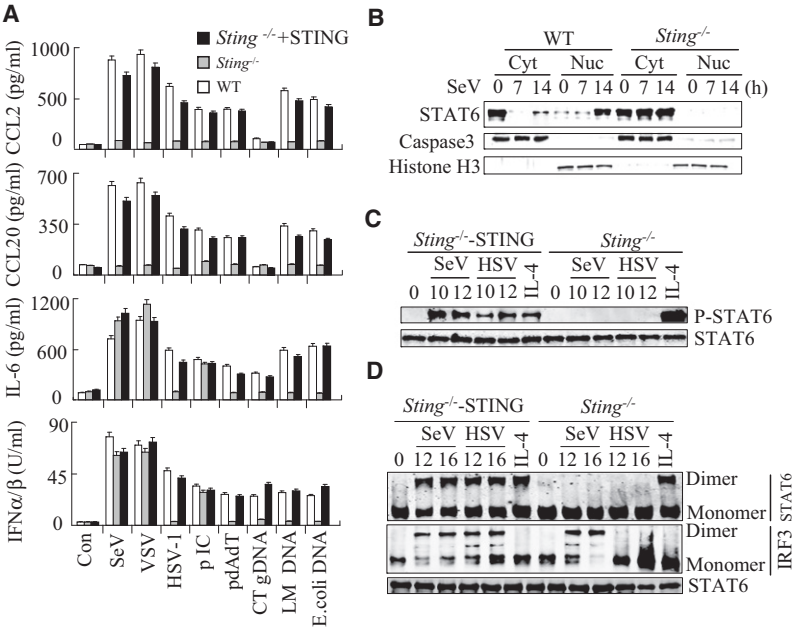

Figure 4. STING Is Required for Virus-Induced STAT6 Activation

(A) ELISA analyses of cytokine production and type I IFN bioassay in WT, *Sting*$^{-/-}$ and *Sting*$^{-/-}$-hSTING MEFs (*STING*$^{-/-}$ MEFs reconstituted with human STING) infected with virus or transfected with poly (I:C)/poly dAdT/genomic DNA from Calf thymus (CT gDNA)/*Listeria Monocytogenes* (LM DNA)/*E. coli*.

(B) Western blot analyses of fractionated WT and *Sting*$^{-/-}$ MEFs infected with SeV for the indicated hours. Cyt, cytosol; Nuc, nucleus.

(C) *Sting*$^{-/-}$ and *Sting*$^{-/-}$-hSTING MEFs expressing human STAT6 were infected with the indicated viruses or treated with IL-4. STAT6 phosphorylation was analyzed by western blot.

(D) Cells in (C) were analyzed by native-PAGE and western blot for dimerization of STAT6 and IRF3.

Data are means ± SEM. See also Figure S4.

To address this possibility, we first assessed the effect of RNAi knockdown of STING. Suppression of STING expression almost completely abolished STAT6 activation in response to SeV infection, but had little effects on IL-4 treatment (Figures S4A–S4C). Meanwhile, the induced interaction between MAVS and STAT6 (Figure S4D) and translocation of STAT6 from cytosol to ER fraction and later to nucleus was barely detectable (Figure S4E). Further evidence for a critical role of STING in virus-derived STAT6 activation showed that *Sting*$^{-/-}$ MEFs lost CCL2/20 induction in response to virus and transfected genomic DNA, although comparable amounts of IL-6 and type I IFNs were detected in response to SeV, VSV, and poly (I:C) (Figure 4A). This result also demonstrated that STING is dispensable for RLR-mediated type I IFN production. As a control, WT and STING-reconstituted *Sting*$^{-/-}$ MEFs showed normal response, highlighting the vital role of STING in virus-induced STAT6 activation. STAT6 from *Sting*$^{-/-}$ MEFs retained in the cytosol after virus infection (Figure 4B). Exogenous human STAT6 (hSTAT6) was not phosphorylated on Y^{641} (Figure 4C), nor did it dimerize (Figure 4D) in *Sting*$^{-/-}$ MEFs after virus infection. These data as a whole indicated that STING is required for virus-induced STAT6 activation.

MAVS Is Required for STAT6 Activation by RNA Virus

Since STAT6 was also localized to MAVS-resident MAM and peroxisomes (Figure 1D), we speculated that MAVS might take a part in STAT6 signaling after virus infection. Indeed, MAVS, RIG-I–N, and Mda5-N (where N denotes N-terminal CARD module) strongly activated STAT6 (Figure S5A), consistent with a role for STAT6 in RNA virus infection. Yeast 2-hybrid assays showed that STAT6 interacted only with STING but not with MAVS or TBK1, each of which could bind STING (Figure S5B). This result suggested that STING may act as a platform that assembles the STAT6 signal complex which includes MAVS in the case of RNA virus stimulation.

To verify this point, we examined virus-induced cytokine production in cells derived from *Mavs*$^{-/-}$ mice. SeV could only induce CCL2/20 secretion in bone marrow-derived macrophages (BMDMs) from WT, but not *Mavs*$^{-/-}$ mice; on the contrary, *Mavs*$^{-/-}$ cells responded normally to HSV-1 (Figures 5A and Figure S5C). Similarly, CCL2/20 production was severely diminished in sera or in organs (lungs and livers) of *Mavs*$^{-/-}$ mice intravenously infected with SeV compared to their heterozygous littermates (Figure 5B). SeV infection, but not HSV-1 infection, resulted in more severe lung pathology, with massive infiltration of monocytes, in WT relative to *Mavs*$^{-/-}$ mice (Figure 5C). In addition, SeV-induced STAT6 nucleus translocation was completely abolished in *Mavs*$^{-/-}$ cells (data not shown). The requirement for MAVS in STAT6 signaling was confirmed by that virus-induced CCL2/20 production was fully restored in human MAVS-reconstituted *Mavs*$^{-/-}$ MEFs (Figure 5D). These data demonstrate that MAVS is required for RNA virus-induced STAT6 activation.

We also investigated the role of STING and MAVS in the canonical STAT6 pathway, and we observed normal CCL11 induction in relevant knockout MEFs in response to IL-4 except *Stat6*$^{-/-}$ MEFs (Figure 5E), suggesting that the canonical STAT6 signaling pathway is intact and is independent of STING or MAVS.

TBK1 Is Required for STAT6 Phosphorylation

Our previous results suggest that individual JAK deficiency has little effect on virus-triggered STAT6 phosphorylation, but it remains to be tested whether simultaneous lack of two or more JAKs would inhibit the process. Using Jak inhibitor Ruxolitinib (INCB 018424) and CP690550, which show specific inhibition of JAK1/2 and JAK3/JAK2, respectively, we found that the inhibitors had little impact on virus-induced STAT6 phosphorylation in U1A cells that is deficient of Tyk2 protein (Figure 6A). Consistently, none of the JAKs was phosphorylated in virus-infected U5A cells while STAT6 phosphorylation persisted (Figure 6B), implying a JAK-independent phosphorylation of STAT6. Interestingly, TBK1, IKKε, and IKKβ overexpression led to obvious shift in the mobility of STAT6 on SDS-PAGE (Figure 6C), whereas

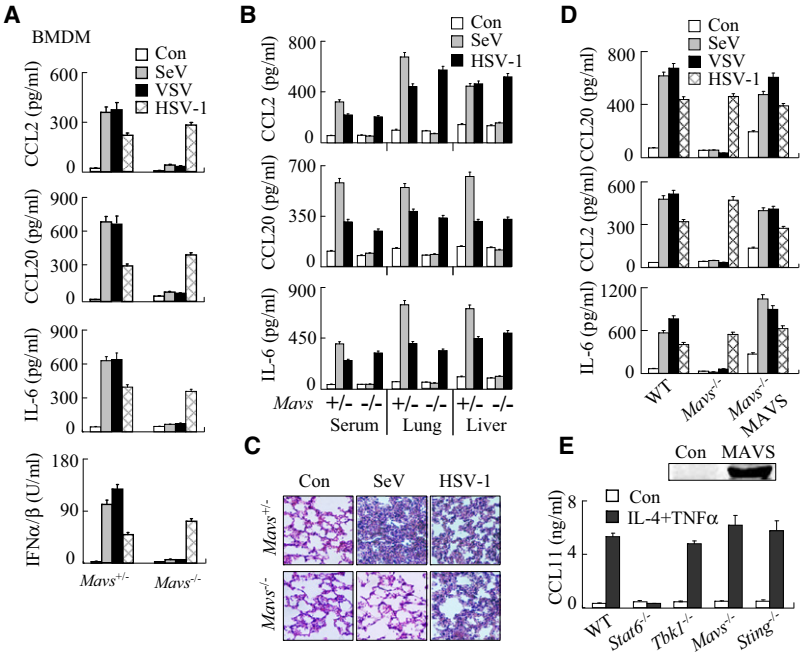

Figure 5. MAVS Is Required for RNA Virus-Induced STAT6 Activation

(A and B) *Mavs*-deficiency impaired STAT6-regulated cytokine production in response to RNA virus. Cytokine production in bone-marrow-derived macrophages (BMDMs) (A) or organs (B) from ~7-week- old *Mavs*$^{+/-}$ and *Mavs*$^{-/-}$ mice (n = 3) infected with the indicated viruses for 24 hr (A) or 48 hr (B).

(C) Impaired pathology of *Mavs*$^{-/-}$ mice in response to RNA virus. Lung sections were made from mice in (B) and stained with hematoxylin-eosin, examined by light microscopy for histologic changes.

(D) Cytokine production in WT, *Mavs*$^{-/-}$ and *Mavs*$^{-/-}$-Flag-hMAVS MEFs infected with the indicated viruses for 24 hr (top). Expression of MAVS was analyzed by western blot with α-Flag (bottom).

(E) TBK1, MAVS, and STING are not required for classical IL-4/13-triggered STAT6 activation. ELISA analyses of CCL11 induction in the indicated MEFs treated with IL-4 (10 ng/ml) and TNF-α (50 ng/ml) for 30 hr.

Data are means ± SEM. See also Figure S5.

no other STATs were affected (Figure S6A), suggesting that STAT6 can be phosphorylated and activated by these kinases, as supported by the observation that TBK1/IKKε promoted STAT6 activation in reporter assays (Figure S6B).

To systematically search for STAT6 phosphorylation site, we individually mutated most of the conserved serines, threonines and tyrosines on STAT6, and found that S^{407}A and T^{572}A showed no response to virus but responded to IL-4/13 perfectly (Figure S6C), indicating that S^{407} or T^{572} might be critical sites in virus-induced but not IL-4/13-induced STAT6 activation. Importantly, S^{407} lies within a consensus motif for TBK1 phosphorylation (Soulat et al., 2008), which was confirmed by in vitro kinase assay (Figure 6E). TBK1 IP-ed from 293 cells infected with SeV was found to phosphorylate STAT6 but not STAT2 or STAT3. Furthermore, phosphorylation of peptide 358–427 was greatly impaired when S^{407} was mutated. Besides, no TBK1 phosphorylation site was indicated in regions 1-358 or 427-610, thus T^{572} is unlikely the target site of TBK1. We also found evidence for the existence of other TBK1 phosphorylation site(s) on the C terminus of STAT6. These data suggest that TBK1 phosphorylates STAT6 in response to virus infection.

Consistently, TBK1 deficiency wiped out STAT6 phosphorylation by poly (I:C) transfection (Figure 6F) and abolished upregulation of STAT6-dependent genes both at the mRNA level (Figure S6D) and the protein level (Figure 6G). Reconstitution of *Tbk1*$^{-/-}$ MEFs with WT, but not kinase-dead TBK1 (KD-TBK1) restored STAT6 activation, emphasizing the importance of TBK1 kinase activity. These data collectively indicate that TBK1 plays an essential role in STAT6 phosphorylation and activation during virus infection.

STAT6 Is Required for Antiviral Immunity In Vivo

Finally we assessed the physiological function of STAT6 using *Stat6*$^{-/-}$ mice and cells. STAT6 was required for virus-, but not TLR-induced CCL2/20 production in peritoneal macrophages (Figure 7A), suggesting that the new activation circuit is restricted to intracellular nucleic acids. Notably, CCL2 production was completely lost in sera and in organs from *Stat6*$^{-/-}$ mice intravenously infected with virus while CCL20 induction was only partially impaired (Figures 7C and 7D), suggesting an absolute STAT6-dependence for CCL2 induction and a partial STAT6-reliance for CCL20 expression. The same was true for macrophages, BMDMs and MEFs (Figures 7A and 7B and Figure S7B).

We also investigated whether virus-induced STAT6 signaling involves other virus-activated transcription factors or components including NF-κB and IRF3. Inhibition of NF-κB by IκB-SR (Brockman et al., 1995) overexpression did not affect virus-induced CCL20 production while slightly reduced CCL2 production (Figure S7A); in parallel experiments, IRF3 deficiency showed no effects at all (Figure 7B). This result indicates that neither NF-κB nor IRF3 is critical for virus-induced STAT6 signaling, suggesting that the bifurcating of STAT6-medieated signaling occurs at an early stage. Data in MEFs and BMDMs from WT, *Il-4r*$^{-/-}$ and *Stat6*$^{-/-}$ mice supported a requirement for STAT6 but not IL-4/IL-4R in virus-induced cytokine production (Figures 7B and 7I and Figure S7B). Severe infiltration of monocytes was observed in the lungs of WT and *Il-4r*$^{-/-}$ mice, compared to no infiltration in those of *Stat6*$^{-/-}$ mice after virus infection (Figure 7E and Figure S7C). In accordance with the above results, virus titer in the lungs and livers of *Stat6*$^{-/-}$ mice was higher than WT controls (Figure 7F), and *Stat6*$^{-/-}$ mice were more susceptible to both VSV and HSV-1 infection (Figures 7G and 7H) than WT and *Il-4r*$^{-/-}$ mice (Figures S7D and S7E). Reconstitution with WT, but not L^{551}A- or S^{407}A-STAT6 restored CCL2/20 production in *Stat6*$^{-/-}$ MEFs after virus infection (Figure 7I), whereas all these forms of STAT6 restored CCL11 production in response to IL-4 (Figure 7J),

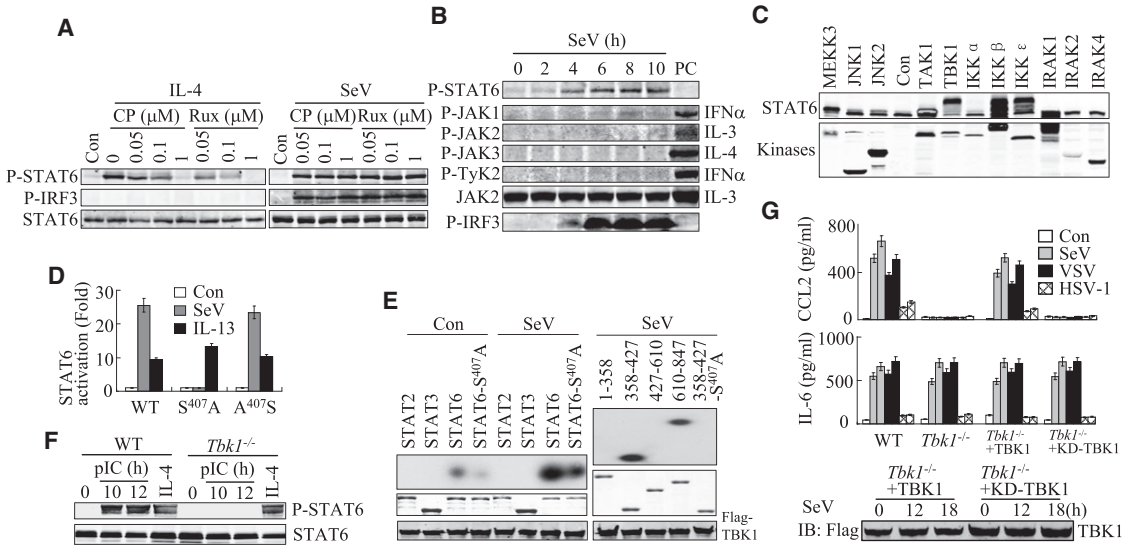

Figure 6. TBK1 Is Required for Virus-Induced STAT6 Activation

(A) SeV-induced STAT6 phosphorylation is JAK-independent. U1A cells untreated or pretreated with JAK inhibitors CP690550 (CP) or Ruxolitinib (Rux) at the indicated concentrations for 4 hr were left untreated (Con), infected with SeV for 10 hr or treated with IL-4 for 2 hr. Phosphorylation of STAT6 and IRF3 was analyzed by western blot.

(B) JAKs are not phosphorylated in U5A cells after virus infection. U5A cells were infected with SeV for the indicated hours. Phosphorylation of STAT6, IRF3 and JAKs was analyzed by western blot. PC, positive control in which 2fTGH cells were treated for 0.5 hr with the indicated cytokines.

(C) TBK1/IKKε and IKKβ overexpression leads to STAT6 mobility change. 293 cells transfected with Flag-STAT6 and the indicated HA-tagged kinases were analyzed by western blot with α-Flag (STAT6, top) and α-HA (kinases, bottom).

(D) STAT6-S^{407} is required for virus-induced STAT6 activation. 293 cells transfected with an E3-Luc and wild-type (WT) or mutant STAT6 were infected with SeV for 24 hr or treated with IL-13 for 12 hr. STAT6 activation was analyzed using luciferase assay (fold induction). $A^{407}S$, the reversed $S^{407}A$.

(E) TBK1 phosphorylates STAT6 on S^{407} in vitro in a virus infection-dependent way. 293 cells expressing Flag-TBK1 were mock-infected (Con) or infected with SeV for 8 hr. Cell lysates were IPed with α-Flag and analyzed by either western blot with α-Flag (bottom) or the kinase assay using the indicated GST-polypeptides as substrates (top). Purified GST-proteins and polypeptides were separated by SDS-PAGE and stained with Coomassie blue (middle).

(F) TBK1 is required for virus-induced STAT6 phosphorylation. WT and *Tbk1*$^{-/-}$ MEFs expressing hSTAT6 were transfected with poly (I:C) or treated with IL-4. STAT6 phosphorylation was analyzed by western blot.

(G) Impaired STAT6-regulated cytokine induction in *Tbk1*$^{-/-}$ MEFs. ELISA analyses of cytokine production in WT, *Tbk1*$^{-/-}$, *Tbk1*$^{-/-}$-TBK1 and *Tbk1*$^{-/-}$-KD-TBK1 (*Tbk1*$^{-/-}$ MEFs reconstituted with kinase-dead TBK1) infected with the indicated viruses. Expression of TBK1 was analyzed by western blot with α-Flag (bottom). Data are means ± SEM. See also Figure S6.

demonstrating that distinct mechanisms are employed by cells to activate STAT6 in response to diverse challenges.

DISCUSSION

The present study shows that STAT6 is activated by intracellular non-self nucleic acids which lead to innate immune activation. STAT6 activated in this manner regulates a specific set of genes that are required for the recruitment of various immune cells to the site of infection. The mechanism employed for STAT6 activation by virus is distinct from that by cytokines like IL-4/13 in the canonical pathway (Figure S7F). Thus, our study identifies a previously unknown STAT6 activating cascade which plays a critical role in innate immunity against microbial infection.

Virus Infection Triggers a Cell Intrinsic Pathway of STAT6 Activation

We have presented several lines of evidence indicating that virus infection triggers a cell intrinsic pathway leading to STAT6 activation. First, STAT6 phosphorylation occurred prior to (or no later than) the phosphorylation of IRF3 and other STATs, supporting a primary response of STAT6 to virus infection. Second, upon virus infection, STAT6-regulated chemokines were upregulated simultaneously with type I IFNs and IL-8. Third, virus-induced STAT6 phosphorylation persisted in cycloheximide- pretreated cells that are unable to carry out protein synthesis. Fourth, condition medium-treated cells showed STAT1/3/5 phosphorylation, but not STAT6 phosphorylation. Fifth, virus-activated STAT6 regulates a specific set of genes involved in immune cell homing; these target genes are different from most of known STAT6-regulated genes. Finally, STAT6 point mutation revealed a distinct activating mechanism employed by cells in response to virus.

Based on the data presented, we proposed a working model for STAT6 activation in response to intracellular nucleic acids (Figure S7F), in which STING plays a central role to integrate signals coming from both RNA and DNA virus infection. Upon DNA virus infection, STING is first activated and then recruits STAT6. TBK1 is also recruited by STING to phosphorylate STAT6 on S^{407}, which in turn activates another unidentified tyrosine kinase to phosphorylate STAT6 on Y^{641}, leading to the homodimerization and nucleus translocation of STAT6. STAT6

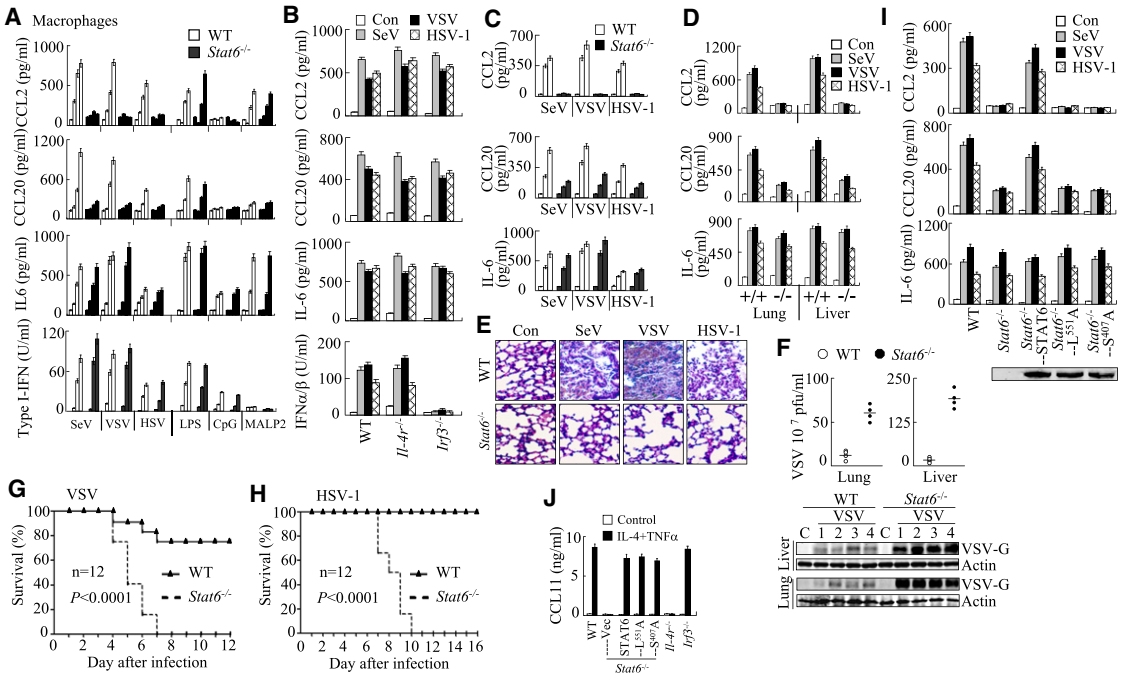

Figure 7. STAT6 Is Required for Antiviral Innate Immunity In Vivo

(A and B) ELISA analyses of cytokine production in peritoneal macrophages (A) and MEFs (B) from WT, *Il-4r*$^{-/-}$, *Irf3*$^{-/-}$ and *Stat6*$^{-/-}$ mice infected with the indicated viruses for 24 hr or treated with CpG DNA, LPS or MALP2 for 6 hr.

(C and D) ELISA analyses of cytokine production in sera (C) and in organs (D) of WT and *Stat6*$^{-/-}$ mice (n = 3) intravenously infected with the indicated viruses for 48 hr.

(E) Impaired pathology of *Stat6*$^{-/-}$ mice in response to virus. Hematoxylin and eosin staining of lung sections from mice in (D).

(F) WT and *Stat6*$^{-/-}$ mice (n = 4) were infected with VSV for 72 hr. VSV titers were determined by standard plaque assays (top). pfu, plaque forming units. Expression of VSV G protein was analyzed by western blot with α-VSV-G (bottom).

(G and H) Survival of ~7-week-old WT and *Stat6*$^{-/-}$ mice intravenously infected with VSV (2×10^7 pfu per mouse) (n = 12, G) or HSV-1 (3.3×10^6 pfu per mouse) (n = 12, H). $p < 0.0001$, *p* values from t test.

(I) Cytokine production in WT, *Stat6*$^{-/-}$, *Stat6*$^{-/-}$-hSTAT6, *Stat6*$^{-/-}$-hSTAT6-L^{551}A and *Stat6*$^{-/-}$-hSTAT6- S^{407}A MEFs infected with the indicated viruses for 24 hr. Expression of STAT6 was analyzed by western blot with α-Flag (bottom).

(J) ELISA analyses of CCL11 production in cells from (I) and other indicated MEFs treated with IL-4 (10 ng/ml) and TNF-α (50 ng/ml) for 30 hr.

Data are means ± SEM. See also Figure S7.

dimer then binds to its target sites to initiate transcription. On the other hand, RNA virus infection triggers STING activation through STING-MAVS interaction on MAVS-resident MAM or peroxisomal membrane; activated STING then dissociates with MAVS, and recruits STAT6 and TBK1, leading to STAT6 activation. Although it remains unclear whether the mitochondrial or the peroxisomal MAVS transmits the signal to STAT6, our results indicate that STING again plays a crucial role during this process.

STAT6 Activation by Virus Differs from the Canonical Pathway

STAT6 activation in response to viral infection is different from that by cytokines through the canonical pathway. First, virus-induced STAT6 activation is JAK-independent, Since the process is normal in individual JAK-deficient cells and is unaffected by treatment with Jak Inhibitors. Critically, in U5A cells virus infection did not induce JAK phosphorylation whereas STAT6 phosphorylation was obvious. Second, STAT6 activation by virus was not initiated by STAT6-receptor interaction, in which SH2 was critical, but by STAT6-STING interaction, in which DBD of STAT6 and C terminus of STING were required. Third, L^{551} is critical only in virus-induced STAT6 activation. The importance of this residue was shown by the observation that L^{551}A interacted with TBK1 constitutively, in a way that probably affected TBK1 phosphorylation of STAT6 (data not shown). Moreover, our studies in STAT2-deficient cells exclude the formation of STAT2/STAT6 heterodimers reported before (Gupta et al., 1999).

Besides Y^{641}, STAT6 also undergoes S^{407} phosphorylation after virus infection. TBK1/IKKε overexpression causes a prominent shift in the molecular weight of STAT6, but no other STATs. TBK1-mediated virus-dependent phosphorylation was confirmed in vitro. Importantly, S^{407}A abrogates STAT6 activation by virus but not IL-4/13, which is also the case in S^{407}A-STAT6 reconstituted *Stat6*$^{-/-}$ MEFs. We believe that virus induces phospho-S^{407} (P-S^{407} for short, see bellow) is prior to P-Y^{641}, based on two findings: 1) S^{407}A-STAT6 underwent P-Y^{641} by IL-4/13 but not virus; 2) IL-4 but not virus induced STAT6 P-Y^{641} in *Tbk1*$^{-/-}$ and *STING*$^{-/-}$ MEFs. The physiological

relevance of S^{407} phosphorylation will be further tested if a STAT6 antibody recognizing this phosphorylated site is available.

Virus induces different STAT6 target genes compared to IL-4/13. We interpret the specificity as a possible result of conformation change in STAT6 dimers that favor distinct target sequences, since S^{407} phosphorylation is unique to virus infection. Also, cofactor(s) may be required that differentially respond to virus and IL-4/13.

Virus-Activated STAT6 Induces Specific Chemokines

Virus triggers STAT6 to induce a set of chemokines capable of attracting various immune cells: CCL2 for monocytes, macrophages and T cells, etc. (Yadav et al., 2010); CCL20 for CCR6-expressing B cells, T cells and dendritic cells; CCL26 for eosinophils, basophils and subsets of NK cells, etc. (Nakayama et al., 2010). Deregulation of these chemokines are involved in diseases associated with the infiltration of immune cells (Boring et al., 1998; Gosling et al., 1999; Harper et al., 2009; Hedrick et al., 2009; Weckmann et al., 2007). Interestingly, CCL2 and CCL20 can be induced by various stimuli including mammalian and bacterial DNA in a TBK1/IKKε-dependent manner (Ishii et al., 2006), but the role of STAT6 in these situations has not been reported. CCL26 is found only in human and is differently regulated by STAT6 in response to IL-4/13 and virus.

We observed much less infiltration of immune cells and higher viral loads in organs of virus-infected *Stat6*$^{-/-}$ mice. Consistently, *Stat6*$^{-/-}$ mice are more susceptible to virus than their WT and *Il-4r*$^{-/-}$ counterparts. The findings explain the hypersensitivity of knockout mice to virus as an outcome of delayed or inadequate immune cell recruitment due to impaired chemokine production (Figures 7E and S7C), supported by abundant cases (Hokeness et al., 2005; Jia et al., 2008).

Recently *Toxoplasma gondii* infection was shown to induce STAT6 P-Y^{641} and activation in HeLa cells independent of IL-4, but the mechanism was unclear (Ahn et al., 2009). Considering that in all tested cells STAT6 can be activated by virus and induces specific genes for immune cell homing, the role of STAT6 on this side now starts to emerge. Moreover, the finding that *Stat6*$^{-/-}$ mice are susceptible to virus infection may shed lights on the function of STAT6 in virus-related immune diseases.

EXPERIMENTAL PROCEDURES

Plasmids, cells, viruses, antibodies, ELISA kits and other reagents used and detailed experimental procedures can be found in Extended Experimental Procedures.

Mice

Stat6$^{-/-}$ mice on a BALB/c background (C.129S2-*Stat6*^{tm1Gru}/J) were purchased from Jackson Labs (Bar Harbor, Me). *Il-4r*$^{-/-}$ mice on a BALB/c background were obtained from Max Delbruck Center for Molecular Medicine as described previously (Li et al., 2008), *Mavs*$^{+/-}$ mice on a 129/Sv/C57BL/6 background were a kind gift from Dr. Zhijian J. Chen. BALB/c mice were purchased from Laboratory Animal Center. Mice were kept and bred in pathogen-free conditions. All animal studies were conducted at the AAALAC-approved Animal Facility in the Laboratory Animal Center of Peking University. Experiments were undertaken in accordance with the National Institute of Health Guide for Care and Use of Laboratory Animals, with the approval of Peking University Laboratory Animal Center, Beijing.

Coimmunoprecipitation, Immunoblot Analysis, Native PAGE, RT-PCR, RNAi, Type I IFN Bioassay, Luciferase Reporter Assay, VSV Plaque Assays, and Subcellular Fractionation

These experiments were performed as previously described (Sun et al., 2009; You et al., 2009).

Yeast Two-Hybrid Screening

The experiment was performed as previously described (Sun et al., 2009). C-terminal human STING (aa 178-379) was used as bait to screen a human leukocyte cDNA library (Clontech, Palo Alto, CA).

Immunofluorescent Confocal Microscopy

The experiments were performed as described (Sun et al., 2009). Imaging of the cells was carried out using Leica TCS SP2 confocal system under a × 100 oil objective.

In Vitro Kinase Assay

The experiment was performed as previously described (Jiang et al., 2002) with minor modification. Human STATs WT or truncation coding sequences were cloned into pGEX-KG. GST protein was purified with glutathione-agarose beads and eluted by glutathione. Purified proteins were examined by SDS-PAGE and Coomassie blue staining. TBK1 immunoprecipitants were incubated with 1 μg purified GST protein in 20 μl kinase buffer containing 10 mM HEPES (pH 7.4), 1 mM dithiothreitol, 5 mM $MgCl_2$ and 5 μCi of γ^{32}P-ATP (3000 Ci/mM) at 25°C for 15 min. Samples were resolved by SDS-PAGE, dried and visualized by autoradiography.

Microarray Analysis

RNA was extracted with Trizol (Invitrogen) and verified with RNA integrity number (RIN). The aminoallyl-RNA (aRNA) probes labeled with NHS-Cy5 (Amersham) were hybridized at 50°C for 16 hr to the Human Whole Genome OneArray TM Version 4.3 (PhalanxBiotech Group, Taiwan), scanned with Axon 4000B Scanner (Molecular Devices, USA) and analyzed with Genepix software (Molecular Devices USA). Array data are available at Gene Expression Omnibus (http://www.ncbi.nlm.nih.gov/geo/) under the accession number GSE26435. Detailed procedures are described in the Extended Experimental Procedures.

Lung Histology

Lungs from control or virus-infected mice were dissected, fixed in 10% phosphate-buffered formalin, embedded into paraffin, sectioned, stained with hematoxylin-eosin solution and examined by light microscopy for histologic changes.

Isolation of MEFs, BMDMs, and Macrophages

Embryonic fibroblasts (MEFs) from WT and mutant mice were prepared from day 15 embryos and cultured in DMEM supplemented with 10% FBS. Bone marrow derived macrophages (BMDMs) were isolated from tibia and femur. Cells were cultured in 10 cm Petri-dish at 37°C for 5 days. At day 3, 5 ml medium (DMEM with 20% FBS, glutamine and 30% L929 supernatant) was added. Peritoneal macrophages were harvested from mice 4 days after thioglycollate (BD, Sparks, MD) injection, and cultured in DMEM supplemented with 5% FBS. Cells were plated into 24-well plates and cultured in the absence or presence of LPS (100 ng/ml), MALP-2 (100 ng/ml) and CpG (100 nM) for 6 hr, or infected with the indicated virus for 24 hr. Cytokine production was analyzed by ELISA or bioassay.

Virus Infection

Cells were infected with SeV (0.1 multiplicity of infection (M.O.I.)), HSV-1(5 M.O.I.) or VSV (1 M.O.I) for 1 h; cells were washed with PBS and cultured in fresh media. Cytokine production was analyzed 24 hr later. For in vivo cytokine production studies, age- and sex-matched groups of mice were intravenously infected with HSV-1 (1.4×10^7 pfu per mouse), VSV (5×10^7 pfu per mouse) or SeV (1 000 TCID 50/ml, 200 μl per mouse).

Statistical Analysis

Student's t test was used to analyze data.

SUPPLEMENTAL INFORMATION

Supplemental Information includes Extended Experimental Procedures and seven figures and can be found with this article online at doi:10.1016/j.cell.2011.09.022.

ACKNOWLEDGMENTS

We thank Drs. Junlin Teng for histological processing; Zhijian J. Chen for *Mavs*$^{-/-}$ mice; George Stark for 2fTGH, U1A-U6A, and γ2A cells; Wen-Chen Yeh for *Tbk1*$^{-/-}$ MEFs and Tadatsugu Taniguchi for *Irf3*$^{-/-}$ MEFs; and Drs. M. Tian and Y. Rao for critical reading of the manuscript. This work was supported by grants from the China Natural Science Foundation (30772024 and 31025010), the Chinese Ministry of Science and Technology (2007CB914502) and the Chinese Ministry of Education (108002). Z.J. designed research; H.C., H.S., F.Y., W.S., X.Z., L.C., J.Y., Y.W., H.T., and Y.G. performed research; W.X., J.G., H.I., D.G., G.B., and Z.Q. contributed new reagents/ analytical tools; H.C., H.S., F.Y., W.S., X.Z., L.C., J.Y., Y.W., H.T., Y.G., and Z.J. analyzed data; and X.Z. and Z.J. wrote the paper.

Received: January 21, 2011
Revised: May 8, 2011
Accepted: September 19, 2011
Published: October 13, 2011

REFERENCES

Ablasser, A., Bauernfeind, F., Hartmann, G., Latz, E., Fitzgerald, K.A., and Hornung, V. (2009). RIG-I-dependent sensing of poly(dA:dT) through the induction of an RNA polymerase III-transcribed RNA intermediate. Nat. Immunol. *10*, 1065–1072.

Ahn, H.J., Kim, J.Y., and Nam, H.W. (2009). IL-4 independent nuclear translocalization of STAT6 in HeLa cells by entry of Toxoplasma gondii. Korean J. Parasitol. *47*, 117–124.

Akimoto, T., Numata, F., Tamura, M., Takata, Y., Higashida, N., Takashi, T., Takeda, K., and Akira, S. (1998). Abrogation of bronchial eosinophilic inflammation and airway hyperreactivity in signal transducers and activators of transcription (STAT)6-deficient mice. J. Exp. Med. *187*, 1537–1542.

Boring, L., Gosling, J., Cleary, M., and Charo, I.F. (1998). Decreased lesion formation in CCR2−/− mice reveals a role for chemokines in the initiation of atherosclerosis. Nature *394*, 894–897.

Brockman, J.A., Scherer, D.C., McKinsey, T.A., Hall, S.M., Qi, X., Lee, W.Y., and Ballard, D.W. (1995). Coupling of a signal response domain in I kappa B alpha to multiple pathways for NF-kappa B activation. Mol. Cell. Biol. *15*, 2809–2818.

Bulanova, E., Budagian, V., Orinska, Z., Krause, H., Paus, R., and Bulfone-Paus, S. (2003). Mast cells express novel functional IL-15 receptor alpha isoforms. J. Immunol. *170*, 5045–5055.

Chiu, Y.H., Macmillan, J.B., and Chen, Z.J. (2009). RNA polymerase III detects cytosolic DNA and induces type I interferons through the RIG-I pathway. Cell *138*, 576–591.

Dixit, E., Boulant, S., Zhang, Y., Lee, A.S., Odendall, C., Shum, B., Hacohen, N., Chen, Z.J., Whelan, S.P., Fransen, M., et al. (2010). Peroxisomes are signaling platforms for antiviral innate immunity. Cell *141*, 668–681.

Elo, L.L., Jarvenpaa, H., Tuomela, S., Raghav, S., Ahlfors, H., Laurila, K., Gupta, B., Lund, R.J., Tahvanainen, J., Hawkins, R.D., et al. (2010). Genome-wide profiling of interleukin-4 and STAT6 transcription factor regulation of human Th2 cell programming. Immunity *32*, 852–862.

Gitlin, L., Barchet, W., Gilfillan, S., Cella, M., Beutler, B., Flavell, R.A., Diamond, M.S., and Colonna, M. (2006). Essential role of mda-5 in type I IFN responses to polyriboinosinic:polyribocytidylic acid and encephalomyocarditis picornavirus. Proc. Natl. Acad. Sci. USA *103*, 8459–8464.

Gosling, J., Slaymaker, S., Gu, L., Tseng, S., Zlot, C.H., Young, S.G., Rollins, B.J., and Charo, I.F. (1999). MCP-1 deficiency reduces susceptibility to atherosclerosis in mice that overexpress human apolipoprotein B. J. Clin. Invest. *103*, 773–778.

Gupta, S., Jiang, M., and Pernis, A.B. (1999). IFN-alpha activates Stat6 and leads to the formation of Stat2:Stat6 complexes in B cells. J. Immunol. *163*, 3834–3841.

Harper, E.G., Guo, C., Rizzo, H., Lillis, J.V., Kurtz, S.E., Skorcheva, I., Purdy, D., Fitch, E., Iordanov, M., and Blauvelt, A. (2009). Th17 cytokines stimulate CCL20 expression in keratinocytes in vitro and in vivo: implications for psoriasis pathogenesis. J. Invest. Dermatol. *129*, 2175–2183.

Hebenstreit, D., Wirnsberger, G., Horejs-Hoeck, J., and Duschl, A. (2006). Signaling mechanisms, interaction partners, and target genes of STAT6. Cytokine Growth Factor Rev. *17*, 173–188.

Hedrick, M.N., Lonsdorf, A.S., Shirakawa, A.K., Richard Lee, C.C., Liao, F., Singh, S.P., Zhang, H.H., Grinberg, A., Love, P.E., Hwang, S.T., et al. (2009). CCR6 is required for IL-23-induced psoriasis-like inflammation in mice. J. Clin. Invest. *119*, 2317–2329.

Hokeness, K.L., Kuziel, W.A., Biron, C.A., and Salazar-Mather, T.P. (2005). Monocyte chemoattractant protein-1 and CCR2 interactions are required for IFN-alpha/beta-induced inflammatory responses and antiviral defense in liver. J. Immunol. *174*, 1549–1556.

Ishii, K.J., Coban, C., Kato, H., Takahashi, K., Torii, Y., Takeshita, F., Ludwig, H., Sutter, G., Suzuki, K., Hemmi, H., et al. (2006). A Toll-like receptor-independent antiviral response induced by double-stranded B-form DNA. Nat. Immunol. *7*, 40–48.

Ishikawa, H., and Barber, G.N. (2008). STING is an endoplasmic reticulum adaptor that facilitates innate immune signalling. Nature *455*, 674–678.

Ishikawa, H., Ma, Z., and Barber, G.N. (2009). STING regulates intracellular DNA-mediated, type I interferon-dependent innate immunity. Nature *461*, 788–792.

Jia, T., Serbina, N.V., Brandl, K., Zhong, M.X., Leiner, I.M., Charo, I.F., and Pamer, E.G. (2008). Additive roles for MCP-1 and MCP-3 in CCR2-mediated recruitment of inflammatory monocytes during Listeria monocytogenes infection. J. Immunol. *180*, 6846–6853.

Jiang, Z., Ninomiya-Tsuji, J., Qian, Y., Matsumoto, K., and Li, X. (2002). Interleukin-1 (IL-1) receptor-associated kinase-dependent IL-1-induced signaling complexes phosphorylate TAK1 and TAB2 at the plasma membrane and activate TAK1 in the cytosol. Mol. Cell. Biol. *22*, 7158–7167.

Kato, H., Sato, S., Yoneyama, M., Yamamoto, M., Uematsu, S., Matsui, K., Tsujimura, T., Takeda, K., Fujita, T., Takeuchi, O., et al. (2005). Cell type-specific involvement of RIG-I in antiviral response. Immunity *23*, 19–28.

Kato, H., Takeuchi, O., Sato, S., Yoneyama, M., Yamamoto, M., Matsui, K., Uematsu, S., Jung, A., Kawai, T., Ishii, K.J., et al. (2006). Differential roles of MDA5 and RIG-I helicases in the recognition of RNA viruses. Nature *441*, 101–105.

Kawai, T., Takahashi, K., Sato, S., Coban, C., Kumar, H., Kato, H., Ishii, K.J., Takeuchi, O., and Akira, S. (2005). IPS-1, an adaptor triggering RIG-I- and Mda5-mediated type I interferon induction. Nat. Immunol. *6*, 981–988.

Kumar, A., Commane, M., Flickinger, T.W., Horvath, C.M., and Stark, G.R. (1997). Defective TNF-alpha-induced apoptosis in STAT1-null cells due to low constitutive levels of caspases. Science *278*, 1630–1632.

Levy, D.E., and Darnell, J.E., Jr. (2002). Stats: transcriptional control and biological impact. Nat. Rev. Mol. Cell Biol. *3*, 651–662.

Li, Z., Jiang, J., Wang, Z., Zhang, J., Xiao, M., Wang, C., Lu, Y., and Qin, Z. (2008). Endogenous interleukin-4 promotes tumor development by increasing tumor cell resistance to apoptosis. Cancer Res. *68*, 8687–8694.

Masuda, A., Matsuguchi, T., Yamaki, K., Hayakawa, T., Kubo, M., LaRochelle, W.J., and Yoshikai, Y. (2000). Interleukin-15 induces rapid tyrosine phosphorylation of STAT6 and the expression of interleukin-4 in mouse mast cells. J. Biol. Chem. *275*, 29331–29337.

Meylan, E., Curran, J., Hofmann, K., Moradpour, D., Binder, M., Bartenschlager, R., and Tschopp, J. (2005). Cardif is an adaptor protein in the RIG-I antiviral pathway and is targeted by hepatitis C virus. Nature *437*, 1167–1172.

Mikita, T., Campbell, D., Wu, P., Williamson, K., and Schindler, U. (1996). Requirements for interleukin-4-induced gene expression and functional characterization of Stat6. Mol. Cell. Biol. *16*, 5811–5820.

Mikita, T., Daniel, C., Wu, P., and Schindler, U. (1998). Mutational analysis of the STAT6 SH2 domain. J. Biol. Chem. *273*, 17634–17642.

Nakayama, T., Watanabe, Y., Oiso, N., Higuchi, T., Shigeta, A., Mizuguchi, N., Katou, F., Hashimoto, K., Kawada, A., and Yoshie, O. (2010). Eotaxin-3/CC chemokine ligand 26 is a functional ligand for CX3CR1. J. Immunol. *185*, 6472–6479.

Quelle, F.W., Shimoda, K., Thierfelder, W., Fischer, C., Kim, A., Ruben, S.M., Cleveland, J.L., Pierce, J.H., Keegan, A.D., Nelms, K., et al. (1995). Cloning of murine Stat6 and human Stat6, Stat proteins that are tyrosine phosphorylated in responses to IL-4 and IL-3 but are not required for mitogenesis. Mol. Cell. Biol. *15*, 3336–3343.

Seth, R.B., Sun, L., Ea, C.K., and Chen, Z.J. (2005). Identification and characterization of MAVS, a mitochondrial antiviral signaling protein that activates NF-kappaB and IRF 3. Cell *122*, 669–682.

Shimoda, K., van Deursen, J., Sangster, M.Y., Sarawar, S.R., Carson, R.T., Tripp, R.A., Chu, C., Quelle, F.W., Nosaka, T., Vignali, D.A., et al. (1996). Lack of IL-4-induced Th2 response and IgE class switching in mice with disrupted Stat6 gene. Nature *380*, 630–633.

Soulat, D., Burckstummer, T., Westermayer, S., Goncalves, A., Bauch, A., Stefanovic, A., Hantschel, O., Bennett, K.L., Decker, T., and Superti-Furga, G. (2008). The DEAD-box helicase DDX3X is a critical component of the TANK-binding kinase 1-dependent innate immune response. EMBO J. *27*, 2135–2146.

Stetson, D.B., and Medzhitov, R. (2006). Recognition of cytosolic DNA activates an IRF3-dependent innate immune response. Immunity *24*, 93–103.

Sun, W., Li, Y., Chen, L., Chen, H., You, F., Zhou, X., Zhou, Y., Zhai, Z., Chen, D., and Jiang, Z. (2009). STING, an endoplasmic reticulum IFN stimulator, activates innate immune signaling through dimerization. Proc. Natl. Acad. Sci. USA *106*, 8653–8658.

Takeda, K., Tanaka, T., Shi, W., Matsumoto, M., Minami, M., Kashiwamura, S., Nakanishi, K., Yoshida, N., Kishimoto, T., and Akira, S. (1996). Essential role of Stat6 in IL-4 signalling. Nature *380*, 627–630.

Takeuchi, O., and Akira, S. (2010). Pattern recognition receptors and inflammation. Cell *140*, 805–820.

Unterholzner, L., Keating, S.E., Baran, M., Horan, K.A., Jensen, S.B., Sharma, S., Sirois, C.M., Jin, T., Latz, E., Xiao, T.S., et al. (2010). IFI16 is an innate immune sensor for intracellular DNA. Nat. Immunol. *11*, 997–1004.

Weckmann, M., Collison, A., Simpson, J.L., Kopp, M.V., Wark, P.A., Smyth, M.J., Yagita, H., Matthaei, K.I., Hansbro, N., Whitehead, B., et al. (2007). Critical link between TRAIL and CCL20 for the activation of TH2 cells and the expression of allergic airway disease. Nat. Med. *13*, 1308–1315.

Wei, L., Vahedi, G., Sun, H.W., Watford, W.T., Takatori, H., Ramos, H.L., Takahashi, H., Liang, J., Gutierrez-Cruz, G., Zang, C., et al. (2010). Discrete roles of STAT4 and STAT6 transcription factors in tuning epigenetic modifications and transcription during T helper cell differentiation. Immunity *32*, 840–851.

Xu, L.G., Wang, Y.Y., Han, K.J., Li, L.Y., Zhai, Z., and Shu, H.B. (2005). VISA is an adapter protein required for virus-triggered IFN-beta signaling. Mol. Cell *19*, 727–740.

Yadav, A., Saini, V., and Arora, S. (2010). MCP-1: chemoattractant with a role beyond immunity: a review. Clin. Chim. Acta *411*, 1570–1579.

You, F., Sun, H., Zhou, X., Sun, W., Liang, S., Zhai, Z., and Jiang, Z. (2009). PCBP2 mediates degradation of the adaptor MAVS via the HECT ubiquitin ligase AIP4. Nat. Immunol. *10*, 1300–1308.

Yuan, Q., Campanella, G.S., Colvin, R.A., Hamilos, D.L., Jones, K.J., Mathew, A., Means, T.K., and Luster, A.D. (2006). Membrane-bound eotaxin-3 mediates eosinophil transepithelial migration in IL-4-stimulated epithelial cells. Eur. J. Immunol. *36*, 2700–2714.

Zhong, B., Yang, Y., Li, S., Wang, Y.Y., Li, Y., Diao, F., Lei, C., He, X., Zhang, L., Tien, P., et al. (2008). The adaptor protein MITA links virus-sensing receptors to IRF3 transcription factor activation. Immunity *29*, 538–550.